第14卷 第2期 CT理论与应用研究 Vol.14 No.2
2005年5月（63~69） CT Theory and Applications May ,2005
Article:1004-4140(2005)02-0063-07

Global Low-Resolution CT Scan Regulated Tomo-synthesis

ZENG Kai, ZHAO Shi-ying, LAURIE Lee Fajardo and WANG Ge
（Micro-CT Laboratory， Iowa Univ.,USA）

Abstract: Tomosynthesis reconstructs a 3D object from a scan consisting of a limited number of projections. Hence, tomosynthesis requires much less radiation dosage as compared to computed tomography (CT). A major problem with tomosynthesis is image artifacts associated with incompleteness of data. In this paper, we propose a tomosynthesis approach to achieve higher image quality in a region of interest (ROI) than competing techniques. First, a low-resolution global CT scan is acquired. Then, a high-resolution local scan is performed with respect to the ROI. Finally, images of the ROI are reconstructed from these two datasets. Our numerical simulation results show that images of the ROI obtained by our approach are significantly better than the counterparts without using the global scan information.

Keywords: Computed Tomography (CT), Micro-CT, Tomosynthesis, local reconstruction, region of interest (ROI).
CLC number: TP301.41 **Document code:** A

基于全局低分辨率CT扫描的合成层析成像技术

曾 凯， 赵世英，Laurie Lee Fajardo[美国], 王 革
（美国爱荷华大学放射学系 显微CT实验室）

摘 要：合成层析成像可由有限几个投影数据重建三维物体，与传统CT相比,该方法所需的射线剂量少得多。由于投影数据不完备，导致的重建图像伪影是合成层析成像的一个主要问题。本文提出一种对感兴趣区域进行合成层析成像方法，和其他方法相比可以得到更好的重建图像质量。该方法首先对目标进行低分辨率全局扫描，然后对感兴趣区域进行高分辨率局部扫描，最后，利用两次扫描的投影数据集合重建感兴趣区域的图像。数值仿真结果表明，用本方法重建感兴趣区域图像，要明显好于没有使用全局扫描信息的方法。

关键词：断面成像， 显微层析成像；合成层析；局部重建；感兴趣区重建

1 Introduction

Tomosynthesis is a technique for reconstructing an object from a series of projections[1]. This area was first initiated by Grant in 1972 , and has been significantly advanced since then [2]. The first type of tomosynthesis algorithms, which are mainly based on a backprojection procedure, suffers from the residual errors in the reconstructed slices. Several algorithms were then proposed to remove these artifacts, such as ectomography[3], selective plane removal[4], and matrix inversion tomosynthesis (MITS) techniques[5]. Nevertheless, due to the incompleteness of data there is always some interference from surrounding structures in the reconstruction. The second type of tomosynthesis algorithms imitates the filtered backprojection (FBP) process widely used in CT. However, the artifacts still exist despite at a less extent [6]. So far, these FBP tomosynthesis algorithms were typically used in the circular scan case.

Since tomosynthesis algorithms cannot do an exact inversion due to incomplete data, iterative methods were developed to achieve better image quality. Over recent years, several iterative algorithms were adapted from CT reconstruction to tomosynthesis, such as algebraic reconstruction techniques (ART) [7], simultaneous-ART (SART) [8], and expectation-maximization (EM) algorithms [9]. Generally speaking, these iterative algorithms produce superior results [10]. Compared with analytic algorithms, iterative algorithms are more powerful to deal

Received date:2005-03-28. This work is supported by NIH grants DC03590, EB002667 and EB004287.

with a limited view scan because prior knowledge or constraints can be effectively introduced in the iterative reconstruction [11], but iterative algorithms are much slower than analytic algorithms [12].

Compared with CT, tomosynthesis can provide 3D images at a much lower dose. Various studies were done on tomosynthesis for major clinical applications, such as mammography [13], chest imaging [14] and dental imaging [15]. However, for high-resolution reconstruction, full-field tomosynthesis still requires a quite high dose. Hence, a local tomosynthesis scan is practically desirable in terms of dosage, but the resultant reduction in projection data will further complicate this reconstruction problem. Not surprisingly, strong gray-level shifting and coupling effects are more evident in the images synthesized from such a local scan.

In this paper, we propose a novel methodology to address the above-mentioned problem by integrating global CT data with local tomosynthesis data, inspired by our previous work on the so-called clinical micro-CT (CMCT) [16]. In our method, a global low-resolution CT (GLCT) scan and a local high-resolution tomosynthesis (LHT) scan are combined to produce image quality that is otherwise not possible. In the following section, we describe our approach in detail. In the third section, we report numerical simulation results. Finally, we discuss relevant issues and conclude the paper.

2 MATERIAL AND METHODS

Here we focus on image reconstruction from a limited number of severely truncated projections utilizing a low-resolution CT scan. The imaging system geometry is shown in Figure 1. In our method, a global low-resolution CT scan (Figure 1(a)) and a local high-resolution tomosynthesis scan (Figure 1(b)) are integrated to reconstruct a ROI. By utilizing the CT scan the local tomosynthesis (Figure 1(b)) can be transformed into a virtual full-field tomosynthesis scan for the ROI (Figure 1(c)). Therefore, with the information from CT data our tomosynthesis can achieve better reconstruction than that without such individualized knowledge.

First, the principle of X-ray imaging is briefly reviewed as follows. If we ignore the statistical fluctuation in X-ray, the attenuated intensity of an X-ray beam obeys (1):

$$I(t) = I_0 e^{-\int_0^t f(\mathbf{s}+\boldsymbol{\theta} t)dt}, \qquad (1)$$

where I_0 is the initial intensity of the X-ray beam, $I(t)$ a measured intensity at $\mathbf{s}+\boldsymbol{\theta} t$, $\mathbf{s}$ the vector for the X-ray source position, $\boldsymbol{\theta}$ a vector in the unit sphere, $f(\mathbf{x})$ the attenuation function of the object. Usually, we refer the integral: $\int_0^{+\infty} f(\mathbf{s}+\boldsymbol{\theta} t)dt$ as the line integral or projection value p, *i.e.*, $I(+\infty) = I_0 e^{-p}$.

Normally, the structures inside a ROI are of our main concern relative to that outside the ROI. We can approximate real projections outside the ROI $p_{syn,ROI}$ by synthesizing them $p_{syn,\sim ROI}$ from the low-resolution CT data, where $\sim ROI$ means that region is out of ROI and syn stands for synthesized projection:

$$p_{t,\sim ROI} \approx p_{syn,\sim ROI}. \qquad (2)$$

If $p_{syn,\sim ROI}$ is synthesized in the same geometry of tomosynthesis, we can obtain un-truncated projection data of the ROI from p_{LHT}, where LHT stands for local high-resolution tomosynthesis scan, t stands for true projection and $p_{syn,\sim ROI}$:

$$p_{t,\sim\mathrm{ROI}} + p_{t,\mathrm{ROI}} = p_{LHT}. \qquad (3)$$

Therefore, we have

$$p_{t,\mathrm{ROI}} = p_{LHT} - p_{t,\sim\mathrm{ROI}} \approx p_{LHT} - p_{syn,\sim\mathrm{ROI}}. \qquad (4)$$

By doing so, we can transfer the truncated tomosynthesis problem to a full-field tomosynthesis problem.

In this feasibility study, our method of choice for tomosynthesis is the transmission EM algorithm[9], because prior knowledge or regularization can be naturally included to improve the incompleteness of the data set. This EM algorithm is based on the Poisson model of the photon count. For each projection i, let W_i be the total number of photons leaving the source and heading toward the detector. Let Y_i be the actual number of photons detected. Clearly, the initial photons may reach the detector with a probability $e^{-\sum_{j\in I_i} l_{ij} m_j}$, where j is the pixel subscript, I_j the set of pixels contributing to projection i, and l_{ij} length of the segment in the projection line i that intersects pixel j. Then, the log likelihood over all projections reduces to (5):

$$\ln g(\mathbf{Y}\text{ì}) = \sum_i \left\{ -d_i e^{-\sum_{j\in I_j} l_{ij} m_j} - Y_i \sum_{j\in I_i} l_{ij} m_j + Y_i \ln d_i - \ln Y_i! \right\}, \tag{5}$$

where $\mathbf{Y}$ and **ì** are vectors whose components are the Y_i and m_j respectively, d_i is the x-ray dose per ray which is equal to $\Delta t_i a_i = I_0$, Δt_i the length of time over which the ith projection is collected, and a_i the source intensity. The projection p in (1) can be expressed by $p_i = \ln(d_i / Y_i) = \ln(I_0 / Y_i)$ with the photon count Y_i. As pointed out in [17], the updating scheme can be written as:

$$\begin{aligned} m_j^{n+1} &= m_j^{\,n} + \Delta m_j^{(n)}, \\ \Delta m_j^{(n)} &= \frac{m_j^{\,n} \sum_i l_{ij} (D_i e^{-\langle l, m^{(n)} \rangle_i} - Y_i)}{\sum_i (l_{ij} \langle l, m^{(n)} \rangle_i D_i e^{-\langle l, m^{(n)} \rangle_i})}. \end{aligned} \tag{6}$$

Finally, the initial guess for the iterative tomosynthesis can be made from the global CT data.

Generally, our algorithm consists of the following steps:

(1) Acquire a global low- resolution CT (GLCT scan) (for example, 10 fold degradation in image resolution relative to what we need);

(2) Acquire a local high-resolution tomosynthesis (LHT) scan (for example, 20 projections over a 60 degree angular range);

(3) Synthesize the virtual scan p_{ROI} *from the GLCT volume according to* p_{LHT} *and* $p_{syn,\sim ROI}$ *(Hence, overlying structures from other planes can be basically eliminated);*

(4) Reconstruct the ROI from p_{ROI} *(Our method of choice in this study is the transmission EM algorithm. Its update formula is given in (5) with the initial value being set to the GLCT result) ,Normally,6-8 iterations are needed in our experiments.*

3 SIMULATION RESULTS

The phantom is defined in http://www.imp.uni-erlangen.de/phantoms/head/head.html. Its left region contains fine structures. Thus, we placed our ROI in that region. The global low-resolution CT data of the phantom was acquired in the geometry summarized in Table 1. Then, the local high-resolution tomosynthesis scan of the same phantom was performed as specified in Table 2. All variables are in mathematical units.

Table 1 Geometry of a low resolution cone beam CT scan.

Detector Array	128^2
Detector Cell	0.0187^2
Source to Origin Distance	8
Source to Detector Distance	9
Number of Projections	180
Reconstruction Grid	128^3
Voxel size	0.0156^3

Table 2 Geometry of a local micro-tomosynthesis scan for left ear.

Detector Array	128^2
Detector cell	0.0034^2
Source to Origin Distance	8
Source to Detector Distance	9
Number of Projections	20
Angular Range	[-30º ,30º]
Reconstruction Grid	128^3
Voxel size	0.0031^3

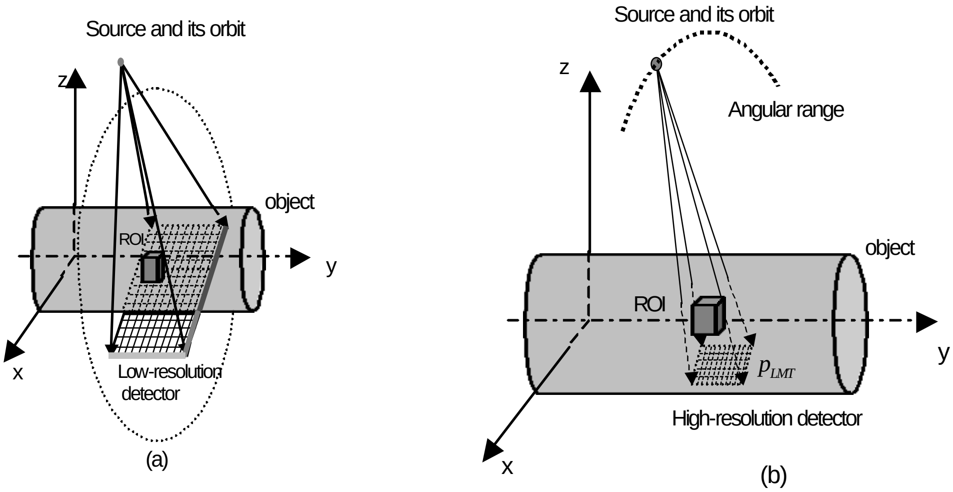

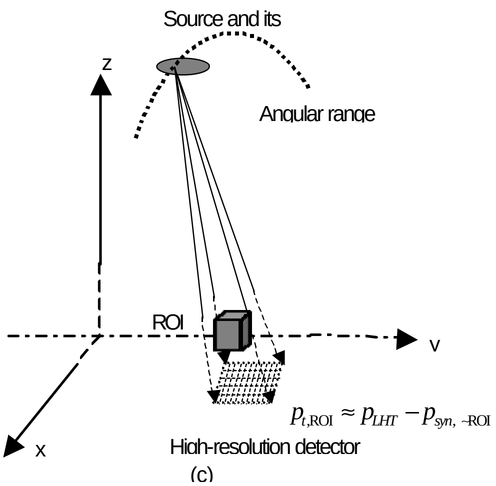

Figure 1 Scan geometries. (a) Global low-resolution cone beam CT scan from which $p_{syn;\,ROL}$ can be synthesized, (b) local high-resolution tomosynthesis scan from which P_{LHT} are acquired. (c) virtual tomosynthesis scan of only ROI whose projection $P_{t,\ tol}$ can be synthesized approximate from (a) and (b).

The reconstructed images from the global low-resolution CT scan are shown in Figure 2. As the resolution is quite low, detailed structures look dramatically blurred. On the other hand, using our new tomosynthesis approach, these structures show very well. Quantitatively, the coupling and shift artifacts are greatly reduced in the integrated tomosynthesis as compared to the direct tomosynthesis, as shown in Figures 3-6.

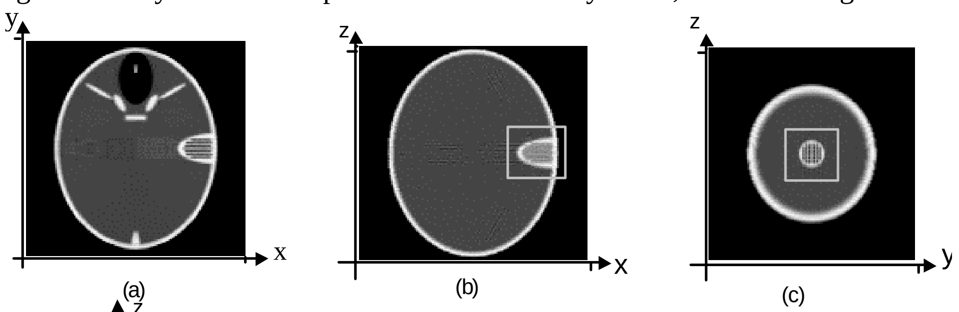

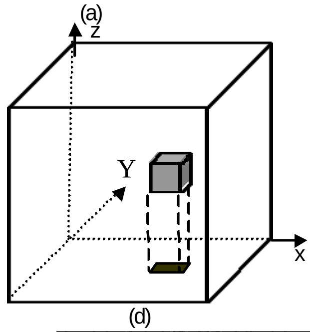

Figure 2 Images from low-resolution cone beam CT reconstruction. Dark rectangles indicate the ROI of left ear. (a) Image in plane: Z=0, (b) image in plane: Y=0, (c) image in plane: X=0.55, and (d) relative positions of left ear ROI. Gray level is set to [0.75,1.85]

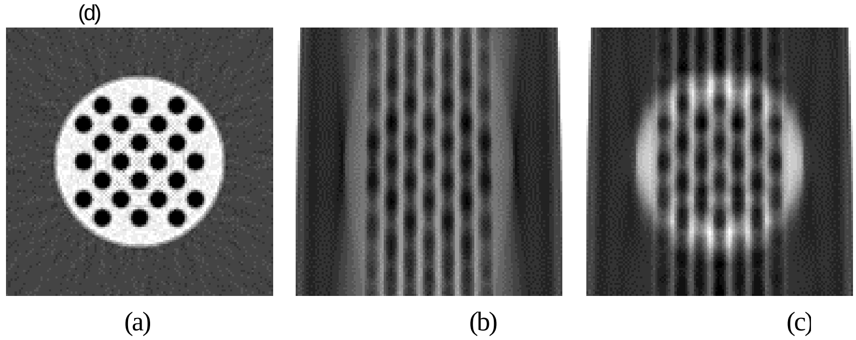

Figure 3 Results from tomosynthesis of ROI according to the geometry of Table 2. (a) high resolution CT image at Plane (x=0.55), (b) result from tomosynthesis by EM algorithm and (c) result from tomosynthesis by EM with the initial value of low-resolution CT data. Gray level window [0.75,1.85]

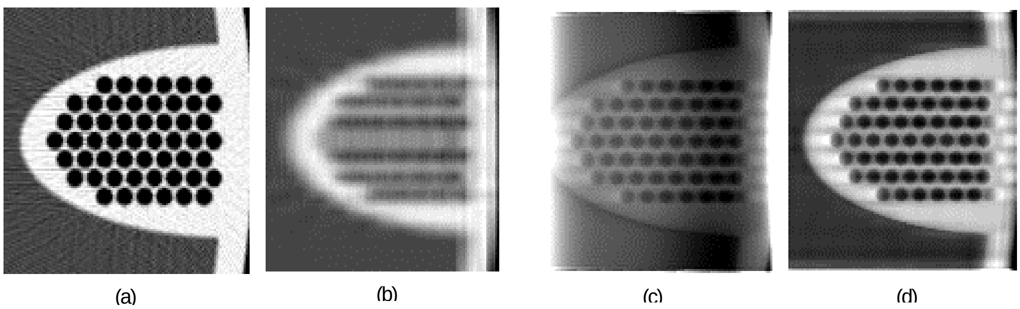

Figure 4 Images of high resolution CT and several reconstruction algorithms in plane: z=0. (a) Head phantom image, (b) image of low-resolution CT data, (c) directly tomosynthesize with EM algorithm, and (d) our tomosynthesis scheme. The gray level of (a), (b) and (d) is set to [0.75, 1.85]. As there are strong shifting effect in (c), its gray level is set to [3.0, 5.5] to show good image.

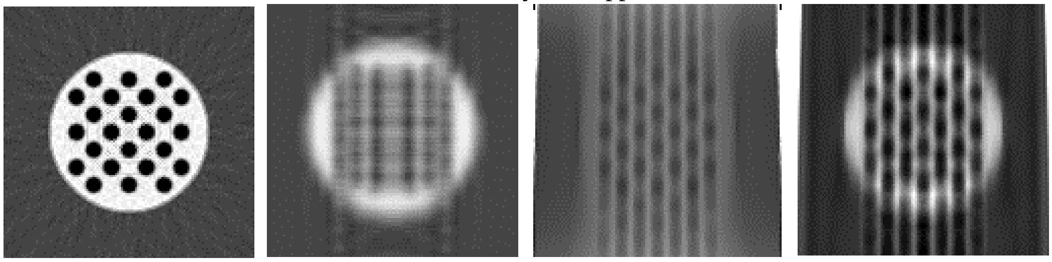

(a) (b) (c) (d)

Figure 5 Images of head phantom and several reconstruction algorithms in plane: x=-0.55. (a) Head phantom image, (b) image of low-resolution CT data, (c) directly tomosynthesize with EM algorithm, and (d) our tomosynthesis scheme. The gray level of (a), (b) and (d) is set to [0.75, 1.85]. As there are strong shifting effect in (c), its gray level is set to [3.0, 5.5] to show good image.

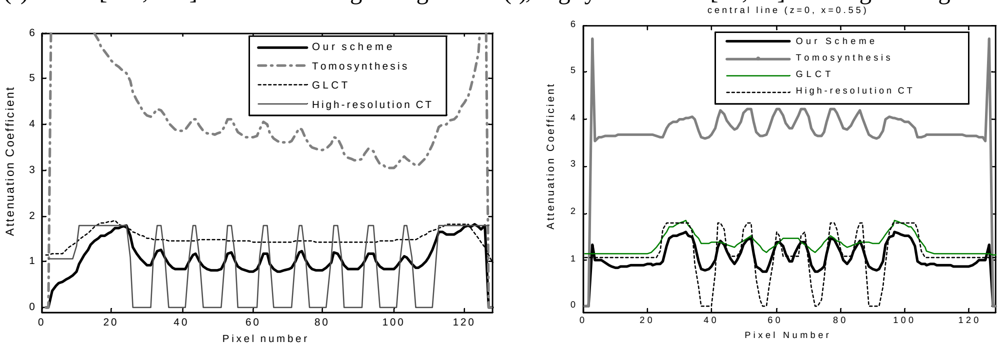

(a) (b)

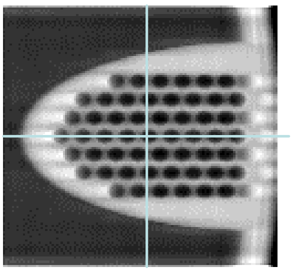

(c)

Figure 6. Line profiles of head phantom and several reconstruction algorithms .
(a) Horizontal line (y=0,z=0), (b) vertical line (z=0,x=0.55), and (c) relative position of the two lines.

4 DISCUSSION AND CONCLUSION

It has been shown in the simulation that our approach effectively eliminates the interference from surrounding structures, and minimizes the shift and coupling effects (Figure 6). Clearly, by integrating global low-resolution CT data with local high-resolution tomosynthesis data, a more accurate local high-resolution reconstruction can be achieved, which is critically important for quantitative analysis. The reason for such an improvement is not difficult to understand. When we perform iterative reconstruction from a limited view scan, the initial value would have a significant influence on the outcome. Because we take advantage of the low-resolution CT data, our method starts with a better guess, producing higher image quality relative to that associated with a normal tomosynthesis.

Also, our local iterative reconstruction method is computationally efficient. Normally, iterative algorithms are not particularly suitable for reconstruction of a ROI since all the voxels are involved in each iteration. However, in our method we form an intermediate virtual scan of the ROI. Consequently, the voxels that are relevant to the tomosynthesis are restricted to the ROI. Hence, the number of such voxels is reduced by an order of magnitude relative to a normal tomosynthesis, which is translated to a speedup of a similar magnitude.

Although there are some recent cone-beam reconstruction algorithms for exact ROI reconstruction [18], they are subject to severe constraints on the scan geometry; for example, the angular range must be sufficient large. Also, we recognize that the global low-resolution CT scan also delivers a certain amount of dose, but such a scan is often available anyway for medical reasons, such as in the case of temporal bone CT imaging [19]. Furthermore, we plan to evaluate the feasibility that we first perform a global low-resolution tomosynthesis scan instead of a global low-resolution CT scan, which might be beneficial in some clinical applications, such as for dental imaging.

In conclusion, we have developed a tomosynthesis approach to achieve higher image quality in a region of interest (ROI) than competing techniques. Our numerical simulation results have demonstrated that the image quality in the ROI is significantly better using our method than that without using the global scan information.

Acknowledgment This work is partially supported by Foundation NIH grants DC03590, EB002667 and EB004287.

References:

[1] Grant D G., Tomosynthesis: a three-dimensional radiographic imaging technique[J]. IEEE Trans Biomed Eng, 1972. **19**(1): p. 20-8.

[2] Dobbins J T, and Godfrey D J. Digital x-ray tomosynthesis: current state of the art and clinical potential[J]. Phys Med Biol, 2003. **48**(19): p. R65-106.

[3] Petersson, C U, et al . Ectomography--a new radiographic reconstruction method--II. Computer simulated experiments[J]. IEEE Trans Biomed Eng, 1980. **27**(11): p. 649-55.

[4] Ghosh Roy D N., et al.. Selective plane removal in limited angle tomographic imaging[J]. Med Phys, 1985. **12**(1): p. 65-70.

[5]Godfrey D J., Rader A and Dobbins J T III. Practical strategies for the clinical implementation of matrix inversion tomosynthesis (MITS). in Medical Imaging 2003[J]: Physics of Medical Imaging, Feb 16-18 2003. 2003. San Diego, CA, United States.

[6] Stevens G M., Fahrig R, and Pelc N J. Filtered backprojection for modifying the impulse response of circular tomosynthesis[J]. Med Phys, 2001. **28**(3): p. 372-80.

[7] Gordon R, Bender R ,and Herman G T. Algebraic reconstruction techniques (ART) for three-dimensional electron microscopy and x-ray photography[J].J Theor Biol, 1970. **29**(3): p. 471-81.

[8] Andersen, A H, and Kak A C. Simultaneous algebraic reconstruction technique (SART): a superior implementation of the art algorithm[J]. Ultrason Imaging, 1984. **6**(1): p. 81-94.

[9] Lange K and Carson R. EM reconstruction algorithms for emission and transmission tomography[J]. Comput Assist Tomogr, 1984. **8**(2): p. 306-16.

[10] WU T., et al.. A comparison of reconstruction algorithms for breast tomosynthesis[J]. Med Phys, 2004. **31**(9): p. 2636-47.

[11] Delaney A H and Bresler Y. Globally convergent edge-preserving regularized reconstruction: an application to limited-angle tomography[J]. 1998. **7**(2): p. 204.

[12] WU T., 3D Mammography Reconst.Using Low Dose Projection Images, in Department of Physics[D]. 2002, Brandeis Univ., p.103.

[13] WU T., et al.. Tomographic mammography using a limited number of low-dose cone-beam projection images[J]. Medical Physics, 2003. **30**(3): p. 365-380.

[14] Dobbins J and Godfrey D. Tomosynthesis imaging of the chest[J]. Medical Physics, 2003. **30**(6): p. 1369-1369.

[15] Ziegler C .M., et al.. Digital tomosynthesis-experiences with new imaging device for dental field[J]. Clin Oral Investig, 2003. **7**(1): 41-5.

[16] WANG Ge , S Z.,YU Hengyong and A.P. Miller C M, Bruce Gantz, Jay Rubinstein. Design, Analysis and Simulation for Development of the First Clinical Micro-CT Scanner[J]. Radiology (Accepted), 2005.

[17] Lange K and Fessler J A.Globally convergent algorithms for maximum a posteriori transmission tomography[J]. IEEE Trans Image Processing, 1995. **4**(10): p. 1430.

[18] Clackdoyle R., et al.. Quantitative reconstruction from truncated projections in classical tomography[J]. IEEE Trans Nucl Sci 2004. **51**(5): p. 2570.

[19] Jager L, et al.CT of the Normal Temporal Bone: Comparison of Multi- and Single-Detector Row CT[J]. Radiology, 2005. 235(1): p.133-41

Author Biography: ZENG Kai（1980-），male, he study in Department of Engineering Physics, Tsinghua Univ. got Master degree; from 2004 to now, he studied in Micro-CT Lab, Iowa Univ. for Ph D study, his research is mainly on 3D-CT reconstruction & tomosynthesis , Up to now he has published 9 scientific articles in China and United States.

曾凯，男，2002－2004年在清华大学工程物理系，从事锥形束三维CT的重建算法研究，2004年获硕士学位。